

## Megavoltage bremsstrahlung end point voltage diagnostic

T. Feroli,<sup>1</sup> M. S. Litz,<sup>1</sup> G. Merkel,<sup>1</sup> T. Smith,<sup>1</sup> N. R. Pereira,<sup>2,a)</sup> and J. J. Carroll<sup>3</sup>

<sup>1</sup>Army Research Laboratory, 2800 Powder Mill Rd., Adelphi, Maryland 20873, USA

<sup>2</sup>Ecopulse, Inc., P.O. Box 528, Springfield, Virginia 22150, USA

<sup>3</sup>Youngstown State University, Youngstown, Ohio 44555, USA

(Received 4 September 2008; accepted 22 February 2009; published online 19 March 2009)

In a material, a beam of x rays is accompanied by various kinds of secondary radiation, including Compton electrons from collisions between the x rays and the material's electrons. For megavoltage bremsstrahlung in air, many of these Compton electrons are forward-directed and fast enough to be deflected outside the beam's edge by a magnetic field perpendicular to the beam. At the beam's edge, the dose from the deflected Compton electrons has a pattern that depends on the radiation's end point energy. Dose patterns measured with radiochromic film on a nominally 1 and 2 MV linear accelerator agree reasonably well with the corresponding Monte Carlo computations. With further development, the dose pattern produced outside the beam by such a sweeper magnet could become a noninvasive way to monitor megavoltage bremsstrahlung, when the end point energies are difficult to determine with other methods. © 2009 American Institute of Physics. [DOI: 10.1063/1.3098947]

### I. MOTIVATION

Bremsstrahlung refers to x rays with a well-known energy spectrum, generated by electrons with charge  $e \approx 1.60 \times 10^{-19}$  C accelerated to the energy  $eV_m$  by a voltage  $V_m$  penetrating into a material. The energy spectrum depends somewhat on the material and its thickness but, in all cases, the maximum energy of a bremsstrahlung photon is the end point energy  $h\nu = eV_m$ , with  $V_m$  the end point voltage. The higher the end point voltage, the harder and more penetrating the radiation. Knowledge and control of the end point voltage is therefore important in applications where the radiation must produce a well-defined dose in a particular location such as a tumor.

For relatively soft bremsstrahlung, with  $h\nu$  below a few hundred kilovolts, say, the end point voltage is easily found from the radiation's attenuation in a suitable filter. The kVp meters that are standard in medical practice do it this way. However, as the end point voltage increases beyond about 1 MeV, multiple filters and increasingly precise dosimetry are needed to make the end point measurement reliable,<sup>1</sup> and for megavoltage bremsstrahlung differential filtering becomes less and less effective in determining end point voltages above a few megavolts. When the end point voltage is of secondary interest and the radiation's attenuation is the primary concern, as in medical applications, it is standard to measure the dose in water as function of depth directly. For the physics application that motivates the work here, the depth dose is secondary and the end point itself is the important quantity.

This paper describes a way to determine the bremsstrahlung end point energy, with a sweeper magnet. The magnet deflects bremsstrahlung-generated Compton electrons onto a spatially resolved dosimeter parallel to but outside the radiation's path. The same idea was used earlier<sup>2</sup> to measure the

voltage in a high-current pulsed bremsstrahlung generator. The instrument's name, the Compton–Hall (CH) volt meter, comes from the analogy with the Hall effect, wherein a magnetic field across the current moves charge carriers sideways just as the sweeper magnet does with the radiation's Compton current.

There are, of course, other ways to find the end point voltage of bremsstrahlung. Submegavolt bremsstrahlung is often made with a dc voltage  $V$  that accelerates electrons through a vacuum so that measuring  $V$  is tantamount to finding the end point voltage. For higher voltages, a dc potential is so difficult to maintain that the dominant way to make megavoltage bremsstrahlung is with linear accelerators, linacs. These accelerate electrons with electromagnetic fields built up in rf cavities by powerful microwave pulses.<sup>3</sup> The rf power that drives the cavities together with a good model for the interaction between the electrons and the fields then gives the principal energy of the accelerated electrons. On some linacs, electromagnets steer the accelerated electrons in the right direction so that the electron energy can be found from the magnet's current.

The end point voltage comes for free in any diagnostic that measures the entire x-ray spectrum. For the low end, up to photons with a few 100 keV, the Cauchy transmission spectrometer that is widely used in plasma spectroscopy<sup>4,5</sup> has been developed as an absolute standard for medical applications.<sup>6</sup> With enough hard photons, it is sometimes possible to bracket the end point by using the activation threshold of certain nuclei.<sup>7</sup> When the source is weak enough, the energy spectrum can be found directly with highly sensitive nuclear physics instrumentation, e.g., a scintillator photomultiplier or high-purity germanium photon counter coupled to a multichannel analyzer. Bringing the photon flux down to an acceptable level is possible even for linacs, which produce the intense radiation bursts from linacs by scattering off thin foils or other methods including oper-

<sup>a)</sup>Electronic mail: pereira@speakeasy.net.

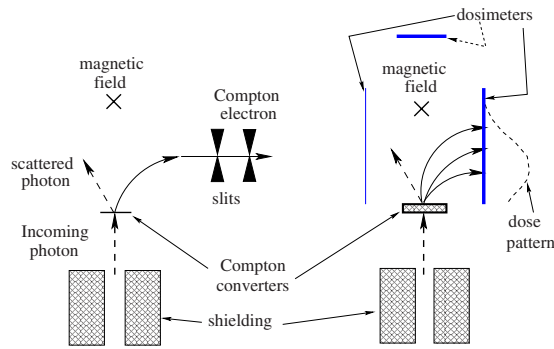


FIG. 1. (Color online) Left: Compton spectrometer based on electron energy. Right: CH geometry. The  $\times$  suggests a magnetic field normal to the figure's plane. The Compton target is thin on the left and thick on the right.

ating the linac in a dark current mode.<sup>8</sup> However, these techniques tend to demand expensive instrumentation and are too difficult for routine use.

When the bremsstrahlung-producing electrons have widely different energies, e.g., in a pulsed discharge with voltage  $V(t)$  and current  $I(t)$ , the time-averaged spectrum  $S(h\nu)$  is an integral over monoenergetic electron bremsstrahlung spectra  $s(h\nu, V)$ , each with their own end point voltage  $V$  and weighed by the charge  $dQ=Idt$ . It differs from the bremsstrahlung spectrum produced by a charge  $Q=\int Idt$  at an average voltage  $V_{av}=\int dtI(t)V(t)/Q$  and end point voltage  $V_{av}$ , although the average spectrum might be characterized by an end point voltage defined by  $V_{av}(\alpha)=\{\int dtI(t)\times[V(t)^\alpha/Q]\}^{1/\alpha}$  with  $\alpha$  between 2 and 3 for a given pulse shape. Additional complications come with high intensity beams, when space charge and beam current are strong enough to make electrons impact the anode at non-normal angles. Such complicating effects can be compensated, to some degree, by not measuring the bremsstrahlung spectrum head-on but at an angle.<sup>2</sup>

Spectrometers that depend on the known bremsstrahlung shape, such as the differential filters mentioned above, do not work when the spectrum has been modified by processes such as backscatter.<sup>9</sup> The spectrum can then be found by differential filtering combined with a suitable unfolding technique.<sup>10</sup> In principle, the range of differential filter spectrometers could be extended up to many megavolts if a filter for such harder x rays would exist. The CH technique, magnetic deflection of Compton electrons, can be viewed as a filter for megavoltage photons.

Figure 1 summarizes the principle. The figure (left side) suggests a conventional Compton spectrometer, i.e., when the individual particles, photons, or electrons, are measured with conventional counting techniques. A photon with energy  $h\nu$  coming from the bottom (dashed) passes through a thin (Compton) converter foil. After interacting with the material's (mostly free) electrons, the scattered photon leaves the foil with less energy and in a different direction, in the process ejecting a Compton electron (solid line) with a corresponding angle and the leftover energy. Most often the angle and energy of the scattered photon are used to infer the incoming photon's energy, but it is also possible to use energy and angle of the Compton electron. These can be obtained from a magnetic field perpendicular to the plane of the figure

and two slits outside the field. Calorimetry on a subset of electrons<sup>8</sup> is another way to find the electron's energy.

Compton spectrometers that count particles are limited by their count rate. Reducing the radiation flux to the appropriate range is easier when the photons are being counted, but using electrons becomes more attractive when the radiation must be measured by averages such as dose or dose rate: per particle, an electron produces more dose than the corresponding photon because electrons are more readily absorbed. Even so, when the scattering foil is thin the signal from the electrons may still be too low to be practical. The approach here is to increase the signal with a thicker foil, at the cost of losing the analytical connection between the incoming and scattered radiation.

On the right side of Fig. 1 is the geometry in the CH volt meter. In this case the Compton conversion foil is thick enough so that the deflected Compton electrons produce a measurable dose. The maximum number of electrons comes out of the foil when the electrons that are generated at the foil's front have barely enough energy to come out on the back so that any additional material in the foil simply reduces the initial radiation. The radiation is then in charged-particle equilibrium, at least in the part of the foil where the radiation comes in.

What is the optimum foil thickness? The most energetic photon in bremsstrahlung has the end point  $eV_m$  and the maximum energy of Compton electrons produced by this bremsstrahlung is  $eV_m/(1+mc^2/2eV_m)<eV_m$ . The more energetic the electron, the deeper it penetrates into a material, so that no Compton electron penetrates farther than an electron with energy  $eV_m$  or the continuous slowing down approximation (CSDA) range. When the converter is this thick, the diffuse cone of electrons that emerges from the converter's back should have the same shape, which is independent on foil thickness.

The Compton electrons generated in the foil's bulk lose energy and scatter out of their initial direction. Those created close to the front lost all the memory of their initial energy and direction, those electrons scattered from a thin layer on the foil's back side maintain the analytic connections with the incoming photon's energy. In the CH concept the few Compton electrons from the back layer are overwhelmed by the many electrons that come out of the Compton converter's bulk.

Once out of the foil and inside the air behind the foil, the magnetic field bends the electrons out of the radiation path, each according to its own initial direction and with its own curvature. On a spatially resolved dosimeter (thick blue line) the electrons produce a dose pattern: the more energetic an electron, the farther the resulting dose is from the converter. On the other side can be a second dosimeter (thin blue line) that could be used to reduce background effects. A third dosimeter in the path of the direct radiation a little further away can be included for practical reasons, e.g., to verify alignment.

The CH approach can also be viewed as a way for photons and electrons in a fully built-up radiation field to be diagnosed separately. Dosimeters are always surrounded by materials with similar radiation absorption properties,

thereby keeping the dosimeter far away from any boundary between dissimilar materials and guaranteeing that the radiation field is fully built up and the radiation is in equilibrium with the Compton electrons. Otherwise, the primary Compton and other secondary electrons ejected by the radiation from the dosimeter itself are not compensated by similar electrons from the dosimeter's surroundings and the dose deposited in the dosimeter would no longer correspond to charged-particle equilibrium: the dose would be lower if the surroundings produce fewer electrons than the dosimeter and higher if the reverse were true.

In the CH concept the dosimeters at the beam's edges are not in charged-particle equilibrium: they are outside the primary radiation field. Without a magnetic field, a radiation beam still produces dose outside the primary beam, due to the secondaries produced by the primary radiation (which may or may not be in charged-particle equilibrium) and when the beam is mirror-symmetric the dose at the beam's edge is too. The magnetic field in the CH geometry breaks the symmetry only for the charged particles.

Even at atmospheric pressure the electrons with the lowest energies interact so strongly with air molecules that their paths are too short to get out of the beam. In contrast, the collision length for energetic Compton electrons can be larger than the electron's radius of curvature in the magnetic field: these electrons can reach the dosimeter outside the beam on one side. On the other side the dosimeter gets a much smaller dose, from scattered photons. Hence, the dose pattern in the favored dosimeter results from the more energetic electrons in the foil's charged-particle equilibrium, mostly Compton electrons, perhaps accompanied by a few energetic electrons generated by secondary processes.

A Hall probe determines the magnetic field from the Hall voltage that compensates the magnetic field effect on the conductivity tensor. A CH voltage measurement does the opposite. Since the Compton electrons carry charge, they constitute a Compton current that is deflected by the magnetic field, without affecting the electrons' characteristic velocity or the equivalent voltage. Figure 1 sketches what the dose profile in the CH geometry should look like the dashed line on the right side of Fig. 1.

The physical size of the dose pattern is easily estimated. Without collisions, a Compton electron cannot get farther away from the converter foil than a diameter of the electron's circular orbit in the magnetic field or twice the radius of curvature  $r_c = p/eB$ . The more energetic the electron, the larger the electron's momentum  $p = mv$  and the larger  $r_c$ . For megavoltage bremsstrahlung the Compton electrons can be relativistic, with  $\gamma \gg 1$  and momentum  $p = \gamma mv$ . Here  $\gamma = eV/mc^2 + 1$  and  $m$  and  $c$  have the usual meaning, the electron mass and the speed of light. In the ultrarelativistic limit, when  $p = \gamma mc$ , the radius of curvature  $r_c = \gamma mc/eB = V/cB$ . A permanent magnet can easily obtain  $B \approx 0.4$  T and for  $V = 2$  MV the limiting radius of curvature  $V/cB \approx 15$  mm. The characteristic length scale is then on the order of tens of millimeters and this distance is indeed roughly the width of the dose pattern produced by the magnet along the radiation

beam. The higher the voltage, the wider the dose pattern and vice versa: the width of the dose is a measure of the end point voltage.

The actual dose pattern must be computed for each bremsstrahlung end point and the measurement of the end point voltage consists in deciding which of the dose patterns from the computation best matches the measurement. The computations should depend only on a single parameter, the end point energy; hence they must either assume a point source of bremsstrahlung created by unidirectional and monoenergetic electrons or use additional information (e.g., on source size) specific to a particular generator.

Our application is as a simple check on the end point voltages produced by a linear accelerator to be used for irradiating isomeric nuclei.<sup>11</sup> In this case there are only two relevant end point energies. Comparing the computed and measured dose profiles for these two energies confirms the accelerator's proper operation in for the higher energy and identifies a problem with the lower energy.

The CH volt meter hardware is simple and cheap. One prototype used standard Nd-B-Fe magnets as found in old-fashioned disk drives. The dosimeter used so far is radiochromic film, which can be read by a commercially available scanner.

With more sensitive and possibly time-resolved dosimetry that seems the proper direction for further development, the CH volt meter may become a convenient instrument for noninvasive routine monitoring of the end point energy in high energy linear accelerators.

## II. DESIGN COMPUTATIONS

The response of the CH volt meter must be computed with a Monte Carlo photon-electron transport code. Scattering and energy loss of a fast electron passing through a thick foil is caused by multiple small-angle collisions with the material's electrons, whose binding energy is a small fraction of the incoming electrons. The distribution over energy and angle of the outgoing electron in a single collision with a free stationary electron is the well-known Compton collision cross section and when the binding energy is taken into account, the cross section is also known. Multiple collisions lead to a series of integrals for the final distribution over energy and angle, which can be approximated only when the scattering angle and the energy loss per collision is small, in a continuous approximation. The result is a trombonelike probability distribution for the electron and a gradual loss of energy as the electron penetrates deeper into the material that is most conveniently found by a Monte Carlo approach. This simply follows an electron as it scatters through the material, colliding not only with stationary unbound electrons but also with electrons that are bound and even with nuclei.

In principle it is possible to convolve the approximate distribution for each Compton electron with their own spectrum of energies and the corresponding distribution over angles. However, the energy spectrum of the Compton electrons is determined by a second energy spectrum for the bremsstrahlung photons. While it is also possible to approximate the bremsstrahlung spectrum analytically, the convolu-

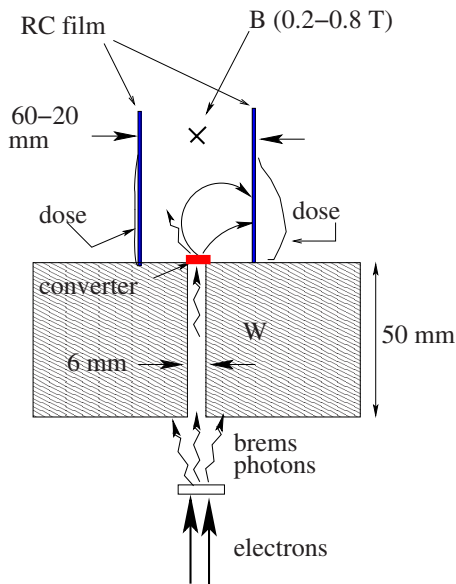


FIG. 2. (Color online) Design of the CH volt meter.

tion of two analytical expressions that are both approximations and must be evaluated numerically in any case makes it logical to sidestep any analytical expressions and use the Monte Carlo approach to compute the entire process, from bremsstrahlung generation, the production of Compton electrons, their transport in the converter, and their passage through the air embedded in a magnetic field until they deposit their energy in the detector. This is contrast to a standard gamma spectrometer, where the angles and energies of both the scattered photon and the Compton electron and the energy of the incoming photon are related by an analytical expression.

The Monte Carlo computations are done with the ACCEPT member of Sandia National Laboratories' most recent ITS code<sup>12</sup> ITS-5. This version's distribution is limited but it has essentially the same physics as the code's standard version (ITS3.1) that is available from the Radiation Shielding Information Center at Oak Ridge National Laboratory. Where needed computations are done in two steps, first computing the bremsstrahlung spectrum from monoenergetic electrons and subsequently using it to compute the resulting doses. The computations confirm and extend what is expected from the simple physics discussed earlier.

The geometry of the CH volt meter in the computations is as in Fig. 2. Energetic electrons hit a bremsstrahlung converter, which is not shown to scale in this figure: it is typically 200 mm away. Some of the bremsstrahlung photons pass through a 6 mm diameter cylindrical hole in a 50 mm thick tungsten shield, after which they interact with a Compton foil or Compton converter (red solid block) that is thick enough to establish charged-particle equilibrium. As in Fig. 1, Compton electrons (thick lines) come out of the foil, in different directions and with different energies. The Compton electron with the larger radius of curvature and the larger energy in the plane of the figure, the lower one in the figure might correspond to the scattered photon suggested in the thin wiggly line. It goes off to the left opposite to its electron. The upper Compton electron in the figure has a smaller ra-

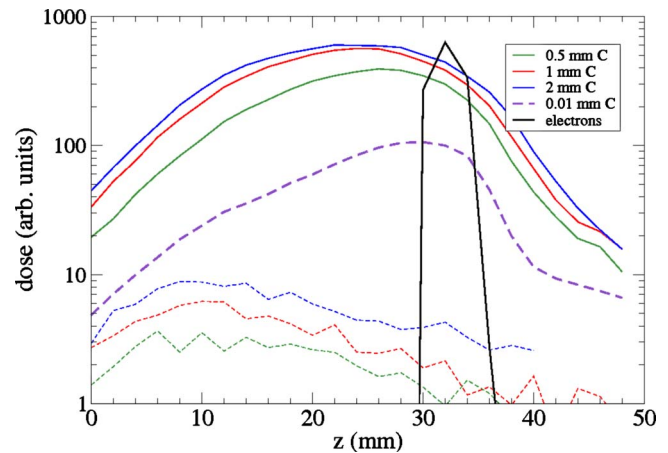


FIG. 3. (Color online) Dose vs distance for monoenergetic electrons with 2 MeV that start at the Compton converter's back side and for 2 MV photons incident on converters with various thicknesses.

dius of curvature and lower energy but it produces a dose farther away from the Compton foil than the other electron. The photon corresponding to this electron, not shown, adds to the dose on the right side. Photons scattering backward do not reach the dosimeter, while the corresponding Compton electrons are the most energetic and go the farthest away from the foil.

In this figure Compton scattering is taken to be perpendicular to the magnetic field so that the Compton electron remains in the plane of the figure. However, almost all Compton electrons move at least partly along the magnetic field and some reach the magnet poles above and below the plane shown. Most of these electrons are absorbed by the poles' iron but a small fraction could scatter back and reach the dosimeter. The same is true for the scattered photon. If it reaches a magnet pole, it could scatter back. The final result is a dose profile with a pronounced peak on the right and on the left a much lower background mostly from scattered photons but with a minor contribution of other electrons or photons that have taken the more convoluted routes.

The Monte Carlo computations that follow have a Compton converter from carbon, but any low atomic number material should give essentially the same result. The measurements are mostly done with the easiest material to use such as aluminum, although it is easier to align the instrument by eye when the converter is optically transparent, plastic, or glass (at least when the collimator seen through the converter is not distorted by the glue that keeps it in place).

For some of the computations, Fig. 2 is to scale but in other computations and measurements the magnetic fields  $B$  may be from 0.2 to 0.8 T and the distance between the dosimeters may be from 60 to 20 mm. In all cases the collimator is a 6 mm diameter hole in a 50 mm thick tungsten block, with the dosimeters and the magnetic field poles forming an elongated rectangular box aligned with the collimator.

The physical description above is further illustrated by Fig. 3. This gives the dose for an electron that comes out of the foil along the normal and compares it to the dose deposited by the plume of Compton electrons that would be generated by a photon with the same energy. The magnetic field

$B=0.2$  T perpendicular to the page bends forward-moving electrons toward the rightmost 50 mm long dosimeter of Fig. 2. The solid lines give the higher doses on the right, the dashed lines are the lower doses in the background dosimeter on the opposite side 20 mm away. The dose is the energy deposited in 2 mm wide and 1 mm thick radiochromic film that is taken to be 50% carbon, 50% oxygen with  $\rho=1$  g/cm<sup>3</sup> as the nominal density. Later computations on the actual hardware used in the measurements include an aluminum backing that is omitted here.

In this and most other figures the computational accuracy is suggested by the wiggles in the lines, almost invisible for the high dose (and numerically around 2%). For the low-dose background, the statistical accuracy is an order of magnitude larger. The dose scale is not used explicitly and therefore left as arbitrary, but it is quantitative. To fit them on the same graph, the dose for an initial electron is reduced 1000 times compared to when the incoming particle is a photon.

As it should, in the code the 2 MeV electron follows a circular orbit through the air behind the foil and hits the side wall as expected from the geometry and its radius of curvature  $r_c \approx 33$  mm. The dose, the solid black line marked “electrons,” is not a point, but a spike that reflects the dose’s spatial resolution (2 mm) and the  $\approx 6$  mm source size. The code includes scattering, but in air at normal pressure the scattering of the 2 MeV electron is almost negligible over tens of millimeters. However, scattering becomes noticeable in a widening of the dose spike by a few millimeters when the air density is ten times too large (due to a misplaced decimal point in the code input).

The few electrons that backscatter from the dosimeter make another orbit in the magnetic field and deposit their energy beyond the point that they could reach otherwise. The dose from such electrons is not visible on the scale of Fig. 3 but it gets onscale if the radiochromic film is replaced by a material with much higher backscatter such as tungsten. These and similar observations from Monte Carlo computations on isolated parts of the CH geometry add insight and confidence to the code results shown later on.

The wide dose patterns shown by the solid lines come from 2 MeV photons that hit the Compton converter’s front side along the normal. The thick dashed line is for a 0.01 mm thin foil. This foil is too thin to slow down or scatter a Compton electron much so that the dashed dose pattern reflects the single-scattering cross section. The three thick converters, with thickness  $d$  equal to 0.5, 1, and 2 mm as marked with the different colors are thick enough to change a Compton electron’s energy and direction. Up to about  $d \approx 0.5$  mm, the dose is roughly proportional to the thickness  $d$  but beyond  $d \approx 2$  mm the dose decreases gradually, consistent with the converter’s photon attenuation. Certainly the 1 mm converter is thick enough for acceptable charged-particle equilibrium: the dose pattern is essentially the same for 1 and 2 mm.

It seems sensible to make the converter thick enough to produce the largest dose pattern, here found to be around 1 mm for 2 MeV end point. The optimal converter thickness will be proportional to the relevant end point energy and for a range of end point energies some intermediate thickness

seems the best. In all cases, though, the dose pattern should be computed for the actual geometry as function of the bremsstrahlung end point energy.

The dose in Fig. 3 beyond the spike at  $r_c$  comes from energetic Compton electrons that leave the foil under an off-normal angle, away from the dosimeter where they eventually end up thanks to the magnetic field. Compton electrons have less energy than the photons that hit them and even a 2 MeV electron could not make dose beyond the dose spike in Fig. 3 from the 2 MeV electron that leaves the Compton converter normally. The opposite is true too. Electrons emitted off-normal toward the dosimeters add to the dose closer to the converter even when their energy exceeds that of a forward-emitted electron. Figure 2 is a projection of two possible orbits for off-normal Compton electrons whose collision plane (as defined by the scattered photon and the electron) is more or less parallel to the plane of the figure.

When the scattering plane is sufficiently out of the plane of the figure, the Compton electron’s helical orbit can end on the magnet poles above and below the plane. At this point the electron starts a new orbit, after backscattering from the magnet. In this computation the magnet is modeled as 1 mm thick iron 10 mm away from the axis, on both sides, so that the Compton electrons come out of the Compton foil into a  $20 \times 20$  mm<sup>2</sup> square box. The collimator’s azimuthal symmetry and the resulting azimuthal symmetry of the Compton current should combine with the mirror symmetry of the dosimeters to make the height  $h$  of the dosimeters another parameter that could affect the dose profile. Since the effect is expected to be small the variation in dose pattern with height has not been explored.

The dashed lines at the bottom of the figure give the dose on the side protected by the magnetic field. They have the same color scheme and order as the solid lines on the high-dose side, where the dose as function of Compton converter thickness  $d$  saturates. However, on the low-dose side the dose is proportional to  $d$ , consistent with a dose generated by photons that are barely attenuated by the Compton converter. The dose for the thinnest Compton converter 0.01 mm, is then too low to show in Fig. 3. The jaggedness in the dose pattern on the low-dose side reflects the statistical scatter.

The computations shown so far intend to clarify the instrument’s principle, hence they use a typical geometry, with unidirectional and monoenergetic electrons or photons that start uniformly against the converter. In the intended application the photon energy is certainly not monoenergetic but follows a typical bremsstrahlung spectrum as in Fig. 4. The solid black line is the photon number spectrum computed in the forward direction for monoenergetic 3 MeV electrons that impact a CSDA-range thick (1.23 mm) tungsten target along the normal. The red dashed line is the number spectrum for monoenergetic electrons with 2 MeV on the same target, as would happen if an x-ray generator designed for 3 MV runs at 2 MV. No photons exceed 2 MeV of course, but away from the end point the spectra for 3 and 2 MV are similar, with a slightly lower peak at slightly lower energy that remains around a few 100 keV. These qualitative fea-

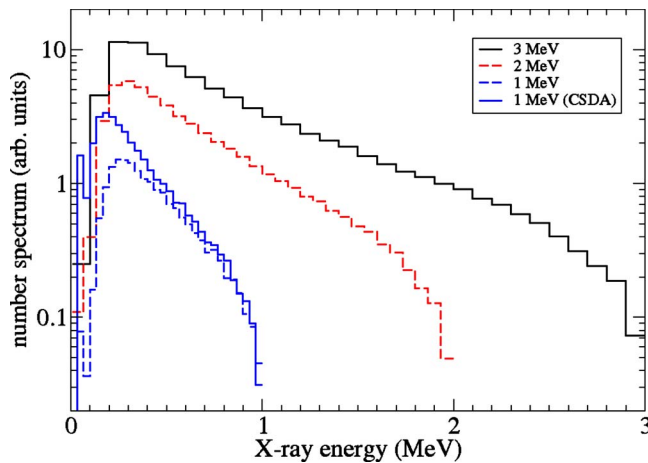


FIG. 4. (Color online) Number spectra for bremsstrahlung made by monoenergetic electrons of 1–3 MV.

tures are also visible in the number spectrum for 1 MeV electrons, the blue line, again computed for the same 3 MV bremsstrahlung target.

The solid blue line is the number spectrum for a tungsten bremsstrahlung target that is no thicker than it has to be, i.e., the CSDA range for 1 MeV electrons (or 0.4 mm). The additional 0.8 mm tungsten in the 3 MV target adds nothing to the bremsstrahlung, but it does attenuate the softer photons as is seen most clearly by the absence of the tungsten fluorescence line at about 60 keV: it is almost completely suppressed by the 3 MV target. The additional tungsten attenuates the softer photons too, up to maybe 200 keV, but the harder part of the spectrum is barely affected. Since the harder photons are most important for the CH volt meter, the computations of its response can therefore start with a pre-computed bremsstrahlung spectrum, irrespective of the bremsstrahlung converter's details. In lieu of the actual converter thickness of the Varian L200A linear accelerator used in the measurements, the computations that follow use spectra computed for 1 and 2 MeV electrons impinging on a  $\approx 10$  mm diameter and 0.84 mm thick tungsten foil, the CSDA range for a 2 MeV electron. This target is then thick enough to stop all primary electrons, so that the target only produces bremsstrahlung photons accompanied by their secondary radiation.

Figure 5 shows the dose computed for the actual geometry of the CH volt meter without a magnetic field. In this prototype instrument the air space behind the converter is 12.6 mm wide, 5.4 mm high, and 26 mm long, with 0.1 mm thick radiochromic film placed against an aluminum backing on both sides. The radiochromic film across the radiation path, see Fig. 1 has no backing. The dose is computed in 1 or 0.5 mm wide bins, along the two sides only.

For 2 MV bremsstrahlung the thick solid black line at the bottom of the figure marked “+” in the legend, gives the dose pattern on one side, the dashed black line the dose pattern on the other side. The two overlap, as they should for this mirror-symmetric situation: the differences are statistical, and illustrate the accuracy of the computations. The red solid and dashed lines are for 1 MV bremsstrahlung. The

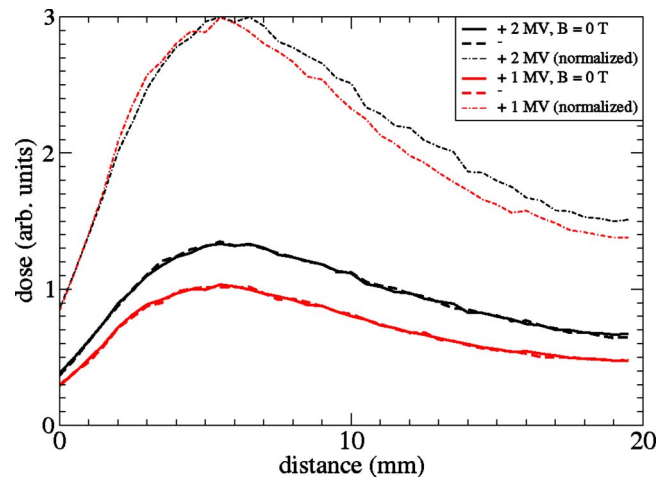


FIG. 5. (Color online) Dose along the side walls from Compton electrons produced by 1 and 2 MV bremsstrahlung without magnetic field.

maximum dose is around unity in the arbitrary units chosen for this figure, while for 2 MV bremsstrahlung the maximum dose is about 1.3 in the same units.

The harder the photons, the more the resulting Compton electrons tend to go forward so that the radiation's end point voltage might be reflected in the dose pattern even without a magnetic field. Such an effect is barely visible in the normalized dose patterns from 1 and 2 MV bremsstrahlung, the thin upper dashed lines marked with “normalized” in the legend. For 1 MV bremsstrahlung the dose pattern is indeed slightly closer to the Compton converter than for 2 MV bremsstrahlung, but the difference is too small to infer the end point voltage from it. The magnetic field is necessary.

Figure 6 is the dose in the CH volt meter computed for 2 MV bremsstrahlung in the same geometry as in Fig. 5 for two magnetic field strengths. When the magnetic field is too low  $B=0.2$  T, the dose on the favored side (black solid line) has a broad peak (in these arbitrary units around 4), about 7 mm away from the Compton converter's back side at  $z=0$ . The non-negligible dose on the electron-deprived side (dashed black), about 1/8 of the peak on the electron-favored side, shows that in this geometry  $B=0.2$  T cannot force all Compton electrons toward the intended side only. A stronger

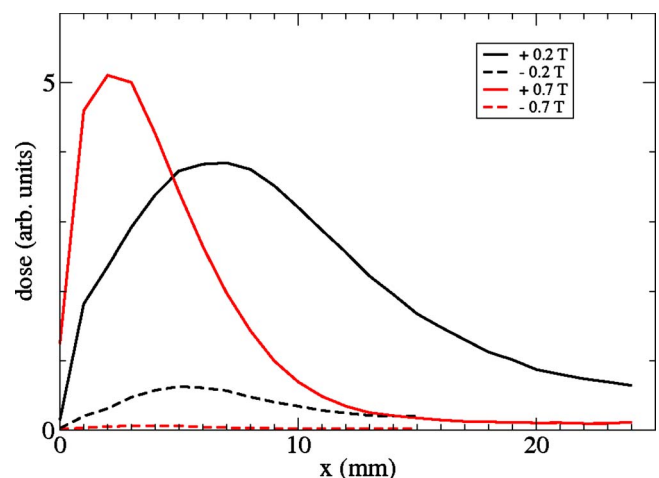


FIG. 6. (Color online) Dose along the side walls from Compton electrons produced by 2 MV bremsstrahlung for the magnetic fields indicated.

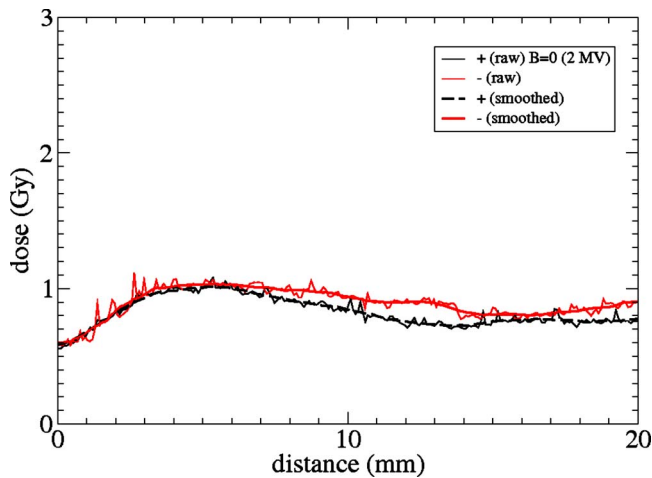


FIG. 7. (Color online) Dose along the path of 2 MV radiation without magnetic field.

field,  $B=0.7$  T (red solid line), gives the peak in the dose at 2 mm, as expected from the decrease in the radius of curvature  $r_c \propto B^{-1}$  with increasing magnetic field. The stronger field reduces the dose on the electron-deprived side (dashed red) to an insignificant value.

For each bremsstrahlung energy there is a cutoff magnetic field that is sufficient to suppresses the undesired dose, but there is no particular reason to use this minimum since sufficiently strong fields are easily obtainable with permanent magnets. Therefore we did not try to find the minimum field, but used  $B \approx 0.78$  T available from an existing magnet in the measurements that follow.

### III. MEASUREMENTS

The CH volt meter's intended application is to megavoltage accelerators, potentially up to 10 MV. Such accelerators are not yet available at the Army Research Laboratory (ARL), but the CH volt meter prototype could be demonstrated with another x-ray generator at ARL, Youngstown State University's 1 and 2 MV linear accelerator. The results obtained to date with this machine below, indicate that the measurement concept is viable.

For this test the dosimetry is done with GAFchromic EBT radiochromic film. Radiochromic film seemed a convenient option to explore the CH volt meter concept, because the dose pattern can be qualitatively judged by eye and read quantitatively without elaborate instrumentation: an inexpensive scanner is adequate. The film is calibrated over its  $\approx 10$  Gy range by measuring the optical transmission after exposure to the linac's radiation. The dose is obtained by integrating the dose rate from the linac's ionization chamber, whose accuracy had been confirmed earlier with individually calibrated  $\text{CaF}_2$  thermoluminescent detectors (TLD) exposed to a calibrated  $^{60}\text{Co}$  source at the Naval Research Laboratory.

In analogy to the magnetic fieldless computation in Fig. 5, Fig. 7 attempts to verify that the dose patterns on the two sides are identical, within experimental variations when  $B=0$  and the situation is mirror-symmetric. For a nominal electron energy of 2 MeV, the thin black line is the dose as function of distance from the Compton converter along the radiation path on the side where a nonvanishing magnetic

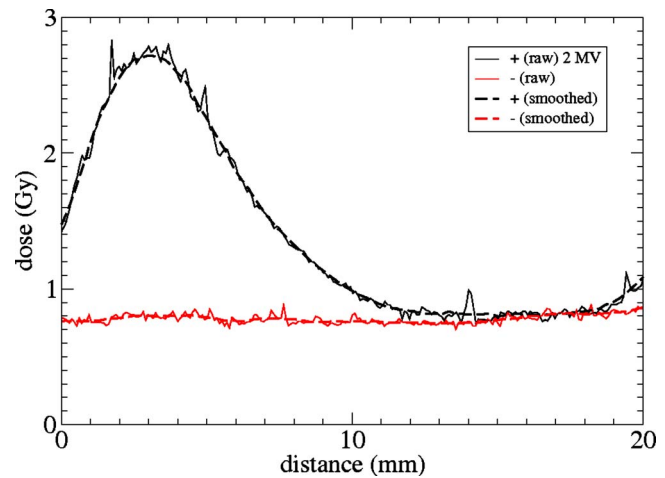


FIG. 8. (Color online) Dose along the radiation path of 2 MV radiation:  $B=0.78$  T.

field would enhance the dose (the + in the legend). The thin red line is the dose pattern on the opposite side, ("−" in the legend). The dose is found by scanning the radiochromic film, integrating the transmission over 2 mm across the  $\approx 5$  mm wide film and converting the optical density into dose according to the film's calibration. The spikes must come from imperfections in the film, perhaps from scratches or other undesirable features introduced by hand cutting the film into thin strips to make them fit between the magnet poles. The spikes disappear in the thicker dashed lines, which give the dose smoothed over 20 individual points along the film.

With  $B=0$  the doses on the two sides are indeed identical, but only up to about 6 mm: the largest difference, beyond 10 mm, is about 20%. The computation in Fig. 6 suggests that the peak dose (at 5 or 6 mm) may be double the background twice or thrice farther from the Compton converter (at 10–18 mm), but in Fig. 7 the signal is at most 130% of the background. The lack of symmetry beyond about 8 mm does not seem to vary in a systematic way with the parameters under the experimenter's control, such as the instrument's alignment with the radiation source or the orientation of the magnetic field. Possible causes include an unintended asymmetry in the radiochromic film's position along the radiation path, or a change in film calibration from excessive bending or twisting as the film is put into place and removed for reading.

In this typical exposure, the dose is just over 1 Gy, which is well within the linear range of the radiochromic film. Here and elsewhere, the exposure continues until the radiochromic film is nicely blue and easy to read. At a 2 MV nominal voltage setting, the linac's nominal dose rate is 30 mGy/s (180 rad/min) 1 m in front of the bremsstrahlung target. In a minute-long exposure the dose on the Compton converter, 250 mm away is then about 30 Gy, resulting in a maximum dose around 3 Gy on the electron-favored side (as in Fig. 8).

A quantitative comparison between measurements and computations was not attempted on purpose. The CH volt meter connects the bremsstrahlung end point to a particular dose pattern that is defined by measuring dose ratios as func-

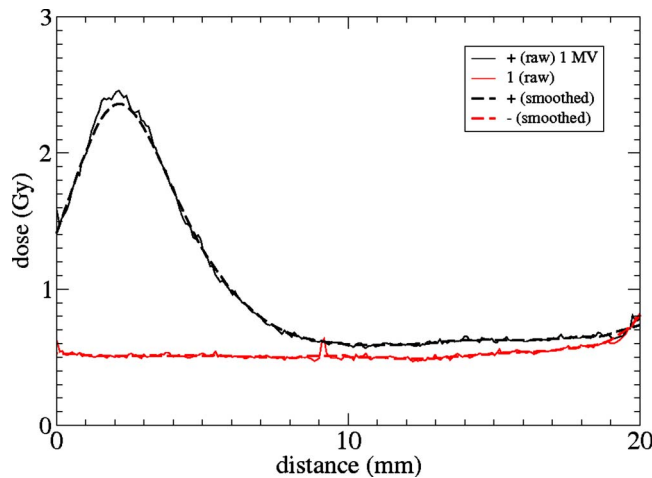


FIG. 9. (Color online) Dose along the radiation path of 1 MV radiation:  $B=0.78$  T.

tion of distance, so that an absolute properly calibrated dose and a quantitative end-to-end comparison with the computations is not necessary

Figure 8 is the dose as function of distance for bremsstrahlung with 2 MV end point and a magnetic field of 0.78 T. The dose on the favored side, in black, shows a clear peak that is very similar to the computations. These were done for the same magnetic field as in the measurement,  $B=0.78$  T (separately from the scoping computations shown earlier). The solid line contains all the points as read from the film (marked “raw” in the legend), again with spikes that disappear after smoothing (the dashed line). The background dose on the opposite side in red, is much lower than the peak. Far enough from the Compton converter the dose is the same on both sides. The increase in dose beyond 20 mm is not expected from the computations done so far, but the substantial dose at the Compton foil itself, at  $z=0$ , is as computed: it is consistent with the circular orbits for the lower-energy Compton electrons, whose diameters  $2r_c$  just fit inside the square air space between dosimeters and magnets. Not shown is the dose for negative  $z$ , nominally behind the Compton converter. In the measurement the film is not flush against the converter so that Compton electrons can reach the film behind the converter’s nominal position. In the computations the converter was slightly larger and against the film.

Figure 9 is the same as Fig. 8 but for 1 MV bremsstrahlung. The figures are qualitatively similar, but with some notable differences: at 2 MV the background is larger compared to the peak (30%) than at 1 MV (20%) and the full width at half maximum of the peak above the background is larger too (about 6 mm versus 4.5 mm). However, it is still possible to estimate the end point voltage by matching the measurements to computations.

Figure 10 compares the measured dose patterns, the thin solid lines in Figs. 8 and 9 and here, with the computed dose from Fig. 6 shown in the dashed lines. Because there is some uncertainty about the exact position of the radiochromic film, the dose patterns are lined up so that their maxima coincide. As a result, the leftmost part of the data is now off the graph. Likewise, the peak dose is scaled so that the computed and measured maxima overlap.

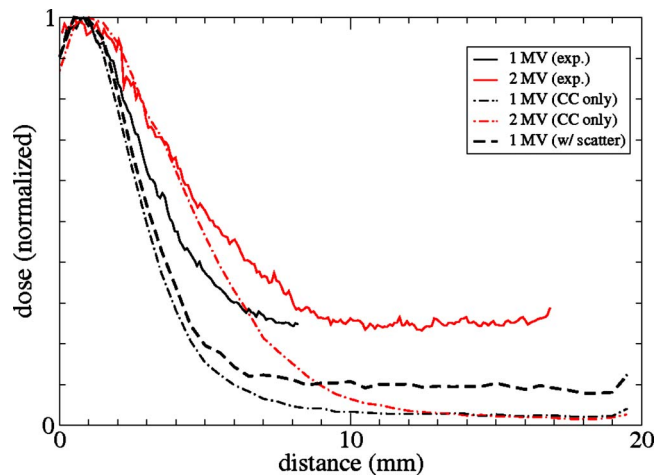


FIG. 10. (Color online) Comparison between the measured and the computed dose for 1 and 2 MV bremsstrahlung.

The (red) solid line for the 2 MV exposure matches the (red) dash-dotted line for the computation reasonably well, at least up to about 5 mm, while farther away from the Compton converter the background is much higher in the experiment than in the computation. In contrast, the (black) solid line from a nominally 1 MV bremsstrahlung exposure, is wider than the computation, the dash-dotted line. Moreover, as with nominally 2 MV bremsstrahlung, the background is too high.

The computed background for 1 MV bremsstrahlung increases with respect to the dose peak when the radiation source in all computations so far, a 5 mm diameter circle flush against the Compton foil that emits photons only along the normal, is replaced by a point source located 200 mm in front of the collimator and 250 mm away from the Compton foil. This source’s photons have an angular spread that illuminates the 50 mm thick tungsten shield over twice the collimator radius, still much more directed than in reality but wide enough to give an order of magnitude increase in computer time (for the few percent statistical accuracy maintained throughout the computations). The resulting background, in the thick dashed line marked *with scatter* in the legend, is now up to  $\approx 10\%$  of the peak and three times larger than with a source against the Compton converter (marked “CC”). The measured background is still twice as large as in the computations so far, up to 20% of the peak. The discrepancy might be narrowed further if the computation were done with the actual source size, which has not yet been measured. Presumably, it is a uniform  $\approx 8$  mm diameter circle, the visible size of the tungsten converter on the linac.

Besides insufficient shielding against radiation scattering from the instrument’s back side, another possible culprit for the remaining discrepancy in the background level may be our failure to achieve the dynamic range that the radiochromic film should be capable of. In these films a large dose is easy to measure because it corresponds to a much reduced transmission of visible light through the film. However, when the dose is low the film’s transparency changes only a little, and such small changes make it difficult to determine low doses accurately. Better results might be obtained by

measuring the film's optical density before the and after exposure on a point by point basis and with the hardware that accommodates a larger piece of film so that the dose can be measured far enough away from the film's edges: the film's response to dose might be affected up to a few mm from the cut.

Other potential problems with hardware implementation should be unimportant. For example, in the Monte Carlo code the magnetic field  $\vec{B}$  in the region behind the Compton converter can be constant and purely transverse,  $\vec{B} = [0, B_y(x, z), 0]$ , thereby violating  $\nabla \vec{B} = 0$  at the magnet's boundaries. Including the fringe fields that satisfy  $\nabla \vec{B} = 0$  at the magnet's boundary make setting up the Monte Carlo computation unnecessarily complicated: in the measurement the Compton converter and the dosimeters are almost completely within the volume where  $\vec{B}$  is constant to within a few percent, as verified with a standard Hall probe. Moreover, any possible variation in strength of the Nd-B-Fe magnets across their surface is smoothed out by 6 mm thick iron pole pieces.

At this moment the suspected reason for the discrepancies is a geometry that may differ from the computation's ideal, in some small way that we have not yet identified. Possibilities include the radiation source, which may not be symmetric or in the center of the tungsten circle to which the collimator is aligned, a Compton foil under a slight angle with the collimator's axis or a twisted dosimeter that has one edge closer to the path of the radiation than the other edge.

It is unfortunate that a separate, independent determination of the radiation's end point voltage could not be done as part of the present test. The dose pattern in Fig. 10 obtained with a nominal setting of 2 MV on the YSU linac agrees well enough with the computations to conclude that the linac indeed produces the intended bremsstrahlung, from electrons accelerated to 2 MeV. However, none of the known or suspected issues with the CH volt meter can make the dose pattern measured for the 1 MV setting wider than what the computation predicts. Since a wider dose pattern corresponds to a higher end point energy, the tentative conclusion is, therefore, that the YSU linac at its 1 MV setting accelerates electrons to a higher energy than intended.

To resolve the various issues discussed so far, it is necessary to do additional measurements with an improved implementation of the CH volt meter, where possible supplemented by one of the alternative techniques for determining bremsstrahlung end point voltages mentioned earlier. One of these could be done recently, using cadmium-111. This nucleus has an activation threshold of 1.2 MeV so that it should not be activated at a nominal 1 MV setting on the linac. However, exposure of a cadmium sample produces a small but measurable amount of radioactivity. This suggests that the linac's end point is slightly higher than 1.2 MV, consistent with the indication from the CH volt meter. This observation is offered with the proviso that the linac was repaired and returned in between the two sets of exposures, and that the linac's end point energy could have changed in the process.

Although the Monte Carlo computations do not yet fully

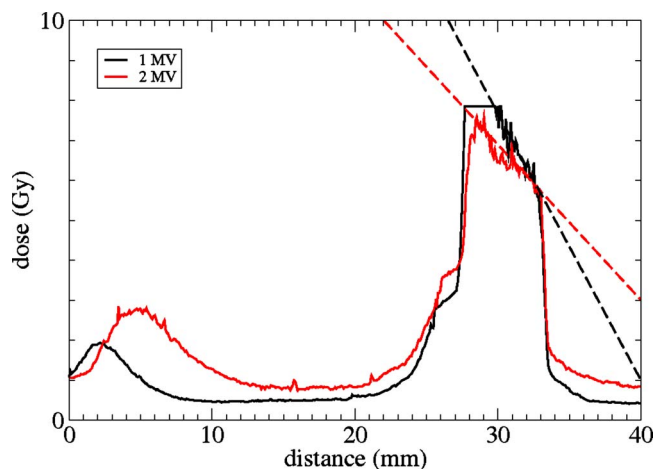


FIG. 11. (Color online) Dose along and inside the path of 1 and 2 MV bremsstrahlung: the magnetic field is 0.78 T.

reproduce the measurements, there are no qualitative surprises in the data shown so far. However, it is interesting to mention that the magnetic field seems to introduce an asymmetry in the dose produced by the direct radiation beam on the radiochromic film in line with the collimator. This asymmetry has not yet been computationally reproduced and was not expected.

The dose patterns discussed so far are along the radiation path. They are measured with two straight pieces of radiochromic film sketched in Fig. 1. In actual fact the two straight pieces are the two ends of a single long strip: the center part of this strip is suggested as the short, horizontal blue bar in Fig. 1. The dose patterns discussed so far are to the side and along the radiation path. When  $B = 0.78$  T the dose made by Compton electrons coming out of the Compton converter cannot be farther than 20 mm behind the converter, as shown in Fig. 9 for 1 MV bremsstrahlung and Fig. 8 for 2 MV bremsstrahlung. There is some dose coming from the beam interacting with the air behind the Compton converter, an interaction that is included in the computations (and does not contribute to explaining the enhanced background discussed earlier). However, the dose farther away from the Compton converter is interesting, in an unexpected way.

Figure 11 shows the dose over an extended region 40 mm, which now includes the dose produced by the direct radiation that passes through the 6 mm diameter collimator and the Compton converter. This radiation gives a  $\approx 6$  mm wide dose peak that connects smoothly with the slight increase in dose around 20 mm already flagged earlier.

The unexpected feature in the straight-through dose is its asymmetry, seen in the gradient across the radiation path, and the fact that the gradient differs for 1 and 2 MV end points. To facilitate comparison the dose for 1 MV (black) has been aligned and reduced on the right side to match the dose for 2 MV bremsstrahlung. The dashed straight lines are drawn through the part of the dose gradient that is unsaturated below about 8 Gy: the 1 MV dose in Fig. 11 exceeded 10 Gy between 28 and 31 mm and is cut off by the software. A minor and possibly significant feature is the slanted step on the peak's left side around 26 mm.

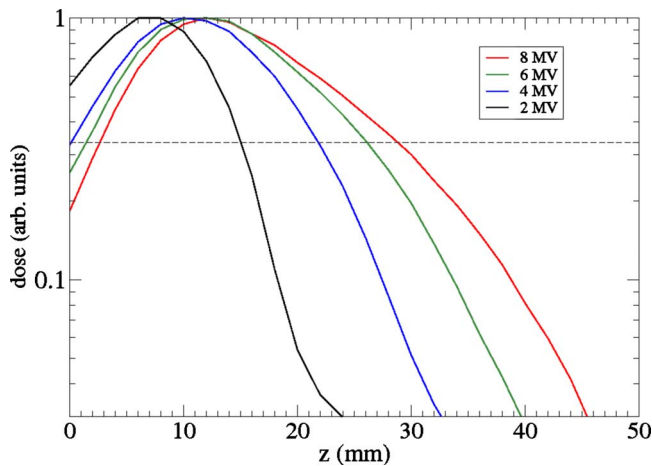


FIG. 12. (Color online) Normalized dose patterns  $D(z)$  computed for multimegavolt bremsstrahlung between  $V=2$  and 8 MV on two sides of a 30 mm wide air space at  $B=0.4$  T.

Without the magnetic field the straight-through dose is symmetric, as it should be and any gradient is too small to see. In fact, the symmetry verifies that the collimator is properly aligned with the radiation source, and alignment was indeed the primary reason for measuring the primary beam's dose pattern, with and without the magnetic field. A satisfactory series of measurements on this unexpected feature was not possible in the available time, but some simple tests excluded a problem with alignment: reversing the magnetic field reverses the gradient.

A Monte Carlo radiation transport computation, with the radiation going through standard pressure air and the usual parameters for high-voltage bremsstrahlung, did not reproduce the gradient highlighted in Fig. 11: this computation did not try to reproduce the dose step between 26 and 27 mm to the left of the peak. It will be interesting to see whether the gradient in the straight-through dose that is unambiguously present in the measurements to date is confirmed in further work, and whether it is caused by an unrecognized quirk in the geometry or appears when additional physics that addresses charged-particle equilibrium in air more in detail is turned on in the Monte Carlo computations.

If the correlation between dose gradient and end point were to be understandable and valid also for higher end point voltages, the dose gradient due to a magnetic field across a radiation beam could possibly become an easier way to find the end point of megavoltage bremsstrahlung than the dose pattern along the beam's edge that is the CH method.

#### IV. EXTENSION TO HIGHER VOLTAGE

For eventual use with the megavoltage linac it may be better to have slightly larger hardware. In the survey computations that follow, the dosimeter on the side wall is 15 mm away from the center of the x-ray beam, while the magnetic field is reduced (to  $B=0.4$  T) to spread the electrons over about 50 mm from the foil. Figure 12 is the result. The peak in the dose shifts away from the Compton converter for bremsstrahlung from 2 to 8 MV and the dose pattern widens as seen before. In this figure the scale is logarithmic, to suggest what might be a more convenient way to measure the

end point voltage than matching the dose profiles: the distance of the half-maximum dose or some other dose ratio. The horizontal dashed line illustrates where the dose is 1/3 of the maximum.

As seen in the previous section, two factors make it difficult to measure the voltage by the position of dose ratios. One is the larger background in the measurements than suggested by these design computations. The idealized source in the computations does not account for off-angle photons that can leak through the collimator, scatter off the collimator inside, and certainly not those that may penetrate insufficient shielding from behind. A second problem could be the limited dynamic range and sensitivity obtained so far from radiochromic film. Moreover, the uncertainty in the position of the radiochromic film with respect to the Compton converter must be addressed by better hardware.

The voltage  $V(t)$  inferred from the normalized dose rate at a single point on a high-dose rate, single-shot bremsstrahlung generator<sup>2</sup> does not suffer from these problems, since in this measurement the diagnostics had a high dynamic range and the instrument is far enough from the source that the photons are reasonably unidirectional.

#### V. CONCLUSION

The dose pattern produced by a sweeper magnet into a well-protected dosimeter along the path of the radiation depends on the end point energy of megavoltage bremsstrahlung. Comparing the dose pattern with computations is then viable way to determine the end point energy. That the method works is confirmed for 2 MV with YSU's L200A Varian linac that is available at ARL, but the machine's nominal 1 MV setting seems to produce higher end point bremsstrahlung.

The dose pattern is registered with radiochromic film, here GAFchromic EBT. The measurements are limited by the film's dynamic range, which in our hands is no better than an order of magnitude. Further work should confirm these results with better hardware, and might further explore whether a magnetic field across a beam of ionizing radiation beam indeed results in a dose gradient at the beam's edge that could be an even more convenient way to find the end point energy.

Another implementation<sup>2</sup> of the same concept but with more elaborate instrumentation successfully measured the electron voltage on a pulsed radiation generator with comparable dose ( $D \approx 4$  Gy at 1 m) but much higher dose rate (around  $\approx 10^8$  Gy/s). In this experiment the voltage was not inferred from a dose profile, but from the radiation's dose rate compared to the dose rate in Compton electrons magnetically swept to one specific point along the radiation path. The 100-fold disparity between the dose rates in these two positions could be compensated by using a more sensitive detector for the Compton-produced dose rate than for the direct radiation: with radiochromic film this could not be done.

The intended application for the CH volt meter is to verify the electron energy produced by a megavoltage linear accelerator that is presently being installed at the Army Re-

search Laboratory. Further work could result in a quality assurance instrument for megavoltage bremsstrahlung that is more convenient to use than the present standard, viz., dose as function of depth in a water phantom.

## ACKNOWLEDGMENTS

We thank Dr. D. Murphy at the Naval Research Laboratory for the TLD calibrations and acknowledge the support for NRP under Contract No. W911QX07C0002 from ARL.

<sup>1</sup>J. C. Riordan, J. E. Faulkner, J. R. Goyer, D. Kortbawi, J. S. Meachum, R. S. Mendenhall, I. S. Roth, and B. A. Whitton, *Rev. Sci. Instrum.* **63**, 4792(1992).

<sup>2</sup>S. B. Swanekamp, B. V. Weber, N. R. Pereira, D. D. Hinshelwood, S. J. Stephanakis, and F. C. Young, *Rev. Sci. Instrum.* **75**, 166 (2004).

<sup>3</sup>C. J. Karzmark, C. S. Nunan, and E. Tanabe, *Medical Electron Accelerators* (McGraw-Hill, New York, 1993).

<sup>4</sup>E. O. Baronova, M. M. Stepanenko, and N. R. Pereira, *Rev. Sci. Instrum.* **72**, 1416 (2001).

<sup>5</sup>L. T. Hudson, R. Atkin, C. A. Back, A. Henins, G. E. Holland, J. F. Seely, and C. I. Szabo, *Radiat. Phys. Chem.* **75**, 1784 (2006).

<sup>6</sup>L. T. Hudson, R. D. Deslattes, A. Henins, C. T. Chantler, E. G. Kessler, Jr., and J. E. Schweppe, *Med. Phys.* **23**, 1659 (1996).

<sup>7</sup>J. J. Carroll, D. G. Richmond, T. W. Sinor, K. N. Taylor, C. Hong, J. D. Standifird, C. B. Collins, N. Huxel, P. von Neumann-Cosel, and A. Richter, *Rev. Sci. Instrum.* **64**, 2298 (1993).

<sup>8</sup>H. I. Amols, A. Rubin, and R. A. Peck, *Nucl. Instrum. Methods Phys. Res. A* **227**, 373 (1984).

<sup>9</sup>N. R. Pereira, *J. Appl. Phys.* **57**, 1445 (1985).

<sup>10</sup>S. C. Gorbics and N. R. Pereira, *Rev. Sci. Instrum.* **64**, 1835 (1993).

<sup>11</sup>J. J. Carroll, *Laser Phys. Lett.* **1**, 275 (2004).

<sup>12</sup>J. A. Halbleib, R. P. Kensek, G. D. Valdez, S. M. Seltzer, and M. J. Berger, *IEEE Trans. Nucl. Sci.* **39**, 1025 (1992).